Publishing House
AKAPIT

COMPUTER METHODS IN MATERIALS SCIENCE

Informatyka w Technologii Materiałów

Vol. 6, 2006, No. 3-4

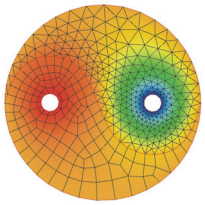

FORMING LIMITS OF AUSTENITIC STAINLESS STEEL SHEETS

A.S. KORHONEN, T. MANNINEN, K. KANERVO

Helsinki University of Technology, P.O. Box 6200, 02015 HUT, Finland
Corresponding author: asko@hut.fi (A.S. Korhonen)

Abstract

The forming limits of austenitic stainless steel sheets were studied. It was found that the observed limit of straining in stretch forming, when both of the principal stresses are positive, is not set by localized necking, but instead by shearing fracture in the through thickness direction. Thus, the Marciniak-Kuczynski type of analysis, which has recently been successfully applied to both low-carbon steels and aluminum, may not apply to austenitic stainless steels. It appears that the forming limits of austenitic stainless steels may be predicted fairly well by using the classical localized and diffuse necking criteria developed by Hill. The fracture criterion of Ritchie and Thompson seems to overestimate the fracture limit. Better models are needed for the work hardening and to develop better limit strain criteria, since the work hardening seems to depend strongly on both strain rate and temperature. The formability of austenitic stainless steels appears to remain good even when coated with hard TiN, although unavoidable cracks will appear with continuing straining.

Key words: sheet metal forming, forming limit diagram, austenitic stainless steels, necking, fracture

1. INTRODUCTION

When finite element (FE) codes moved from research to the production floor in the car industry in the mid-1990s (Makinouchi et al., 1998), the need for more accurate material models became increasingly evident. Without a proper constitutive model, sheet metals are no longer accepted by the car industry and their producers are hard pressed to develop better models. In addition to models describing the initial yielding and subsequent hardening, others are needed to describe the limits of forming, such as necking, fracture and wrinkling.

Austenitic stainless steels are an exceptional class of materials, which have been used to construct cars since the mid-1930s. Still, despite continuing growth the production of stainless steel amounts to only about 2.5 % of the annual production of carbon steels. Although still rare in the car industry, they offer superior strength associated with good formability and exceptional work hardening ability due to deformation-induced phase transformation. Strength levels from 800 to 2000 MPa may be reached with cold formed commercially available stainless steel sheets (Kemppainen et al., 2002) due to deformation induced phase transformation to martensite during or before forming. In vehicle applications, these newly developed ultra high-strength steels have attracted considerable attention, since they offer great benefits in terms of both weight saving and improved safety (Kemppainen et al., 2002; Kemppainen, 2000, Andersson et al., 2002). They can be produced from the metastable 301LN, 304 or 316 grades either by subsequent cold rolling or simply by allowing them to transform and strain harden during the final forming of the part itself. Even further strengthening by subsequent aging of the formed martensite has been studied (Talonen et al., 2004). The formation of martensite depends strongly on the strain rate and

 ISSN 1641-8581

associated deformation heating (Talyan et al., 1998; Ferreira et al., 2004).

Besides vehicles, new applications of austenitic stainless steels include thin precision strips for telecommunication devices (Manninen et al., 2002), and even superplasticity at elevated temperatures has been demonstrated (Yagodzinskyy et al., 2004). Recently, the high price of nickel has shifted interest to low nickel Cr-Mn-based 200-series austenitic stainless steels, especially in Asian countries. However, these steels do not necessarily possess the formability and corrosion resistance of the traditional 300-series austenitic alloys. They also remain non-magnetic even after cold rolling (ISSF, 2005; Habara, 2004).

To explain the localized necking on the right-hand side of the FLD, the Marciniak-Kuczynski theory based on the inhomogeneity existing in the undeformed sheet is nowadays commonly employed in FE simulation codes. By having a proper form of the yield surface, the localization of the plastic flow takes place faster, and FLDs in rather close agreement with the experimental ones can be obtained. However, the process leading to the failure varies depending on the material.

In this paper the authors review the work carried out over many years. For austenitic stainless steels it appears that the mechanism in stretch forming is inclined shearing in the through thickness direction rather than localized necking, as discussed in greater detail later in this paper. Also austenitic stainless steel sheets coated with hard TiN appear to have some formability and, despite observed cracking, even their corrosion resistance seems to remain fairly good.

2. FORMING LIMIT DIAGRAMS

There is a huge amount of literature on forming limit curves or diagrams. There are several different methods for determining the forming limit diagram (FLD). Comparison of the FLDs and the standardization is therefore difficult. The differences, especially near plane strain ($\varepsilon_2 = 0$), may reach from about 10 to 100 %, depending on what method is used. The topic has recently been briefly discussed by Col (2005). Various testing techniques to deform the specimens and various criteria for the definition of the limit strains have been developed. In methods where the friction between the sheet and the tool is eliminated the strain paths remain straight. These techniques employ hydraulic bulging and tensile tests. The Marciniak method employs a supporting driver blank between the punch and the sheet. The third common method is the Nakajima test, which is based on stretching blanks of different widths with a hemispherical punch. The definition of the forming limit may lead to additional scatter, especially if there is a considerable amount of diffuse necking before a localized neck forms.

The forming limits also appear to depend on many other factors. In some forming processes such as incremental forming (Jeswiet et al., 2005) limit strains from three to ten times, or in electromagnetic forming (Seth et al., 2005) even over twenty times, higher than in conventional sheet metal forming have been reported. Also the strain path has been found to affect the limit strains, which may either increase or decrease (Korhonen, 1978a). To avoid the problem, it has been proposed that stress-based coordinates should be used instead of the common strain-based FLD. It has been claimed that the stress-based forming limits are strain path independent and could therefore be better used in FE simulations (Arrieux et al., 1982; Stoughton, 2002; Kuwabra, 2005; Yoshida et al., 2005). However, there are also problems with stress-based coordinates. Backward calculation of stresses from strains may cause problems since there is internal cracking during diffuse necking and the law of volume constancy no longer holds. Also the constitutive equations consisting of the yield condition and the associated flow rule then cease to be valid. However, recent experiments with thick-walled extruded aluminum tubes have been claimed to support the path independence of the limit curve in stress-based coordinates, if hardening is isotropic (Kuwabra, 2005; Yoshida et al., 2005). Other older rules include the proposal by Müschenborn and Sonne (1975) that the effective limit strain depends only on the final direction of the strain path. Later experiments by Kleemola and Pelkkikangas (1977) supported this proposal. However, this seems just be a special case of the necking criteria, as discussed in more detail by Korhonen (1978a).

2.1. Limit strains in principal strain coordinates

The original idea of the forming limit diagram FLD is based on the work of Keeler and Goodwin, as discussed by Painter and Pearce (1974). However, the concept was conceived already much earlier by Gensamer (1946) and Lankford et al. (1947), who plotted the limit strains in the principal strain coor-

dinates. Later the idea was extended to cylindrical compression tests to obtain limit strains farther away on the left-hand side. The principle is illustrated in Fig. 1.

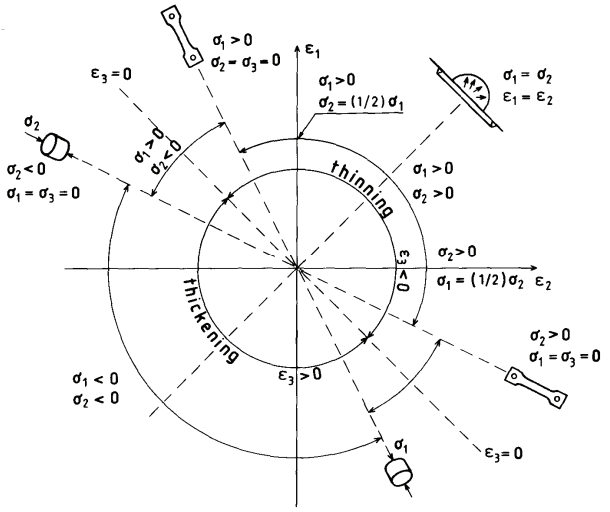

Figure 1. Principle of the FLD measurement.

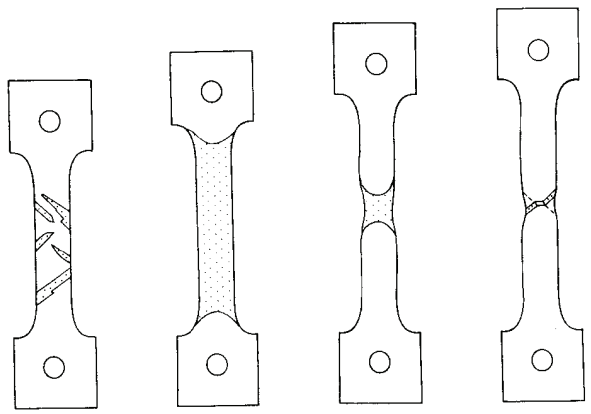

Figure 2. Development of the plastic zone in tensile test.

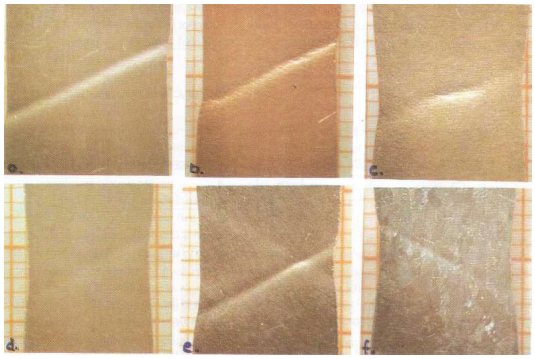

Figure 3. Examples of localized necking in tensile test. a) AlMg3, b) KIE-12-04, c) Ms70-05, d) AISI 304, e) AISI 430 and f) Fe E 350 G (after Korhonen and Eriksson, 1994).

In sheet metal forming, the localized necking limits are usually of main interest. The localization of plastic flow is illustrated schematically in Fig. 2, which shows the case of a tensile test specimen. Figure 3 shows some practical examples on diffuse and localized necking in uniaxial tension for various metals (Korhonen and Eriksson, 1994). The loss of the uniqueness of the solution and subsequent bifurcation of the deformation leads to a shrinking plastic zone or so-called diffuse necking at maximum load. The final localization takes place in a narrow characteristic shear band in the direction of zero elongation. Two sets of such competing shear bands are commonly observed. Fig. 4 shows an example of the Marciniak type of test in deep drawing. Two competing families of localized necks are visible at the bottom of a drawn cup (Korhonen, 1980). The problem, however, is that on the right-hand side of the FLD such shear bands should not exist, since the governing equations are no longer hyperbolic but elliptic, the plane strain being the limiting parabolic case. Even in those cases where thinning is not possible, such as in a compression test of bulk specimens, fracture patterns have been observed to agree qualitatively with the characteristic directions of shearing associated with zero direct strain (Korhonen, 1980).

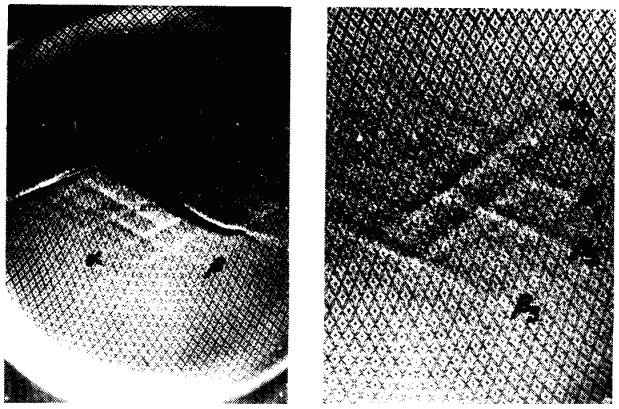

Figure 4. Competing families of localized necks after in-plane stretching of low-carbon steel in a Marciniak-type of test (Korhonen, 1980).

There exists a large amount of literature on both diffuse and localized necking. Theoretically, diffuse necking is associated with the loss of uniqueness of the solution and bifurcation of the flow into the elastic or rigid zone and the shrinking plastic zone. In a series of papers Hill (1957a, 1957b) developed criteria for the uniqueness and stability of plastic flow in rigid-plastic solids. Under all-around dead loading Hill's criterion seemed to coincide with the earlier criterion of Swift, which required a simultaneous load maximum in both principal stress directions (Korhonen, 1978a). For localized necking Hill (1952) had earlier derived another criterion. Since Hill's criterion can not predict the localized necks on the right-hand side of the FLD, Marciniak and Kuczynski proposed the concept of initial inhomogene-

ity in the sheet, which could lead to localization. The concept has been developed further by several authors and it has been shown that if the shape of the yield surface is modified, lower limit strains in closer agreement with the measured ones may be obtained, e.g. for aluminum alloys (Lademo et al., 2004). Further methods for predicting the localized necking limit strains include the assumption of a vertex in the yield surface and application of the J_2 deformation theory instead of the conventional flow theory, as first proposed by Stören and Rice and recently discussed by Chow et al. (2005). Of course the deformation theory applies only to proportional loading and it may therefore not be used to study the strain path effects.

Hill's criteria for both diffuse and localized necking can be written in the form of a simple equation, which is an extension of the well-known Considère construction for the three-dimensional stress space

$$d\bar{\sigma}/d\bar{\varepsilon} = \bar{\sigma}/Z, \tag{1}$$

where the critical subtangent Z for diffuse and localized necking, respectively, can be obtained, according to Hill, from the equations

$$1/Z_d = \frac{\sigma_1(\partial f/\partial\sigma_1)^2 + \sigma_2(\partial f/\partial\sigma_2)^2}{[\sigma_1(\partial f/\partial\sigma_1) + \sigma_2(\partial f/\partial\sigma_2)]\cdot df/d\bar{\sigma}} \tag{2}$$

$$1/Z_l = (\partial f/\partial\sigma_1 + \partial f/\sigma_2)\Big/ df/d\bar{\sigma}, \tag{3}$$

where f is the yield function. As can be seen, both necking criteria depend on the form of the yield condition. For the well-known Hollomon and Voce stress-strain relations

$$\bar{\sigma} = K\bar{\varepsilon}^n \tag{4}$$

$$\bar{\sigma} = B - (B - A)\exp(-n\bar{\varepsilon}) \tag{5}$$

one obtains the following effective limit strains $\bar{\varepsilon}^*$ after substituting them to Eq. (1)

$$\bar{\varepsilon}^* = Zn \tag{6}$$

$$\bar{\varepsilon}^* = (1/n)\ln[(B - A)(Zn + 1)/B]. \tag{7}$$

However, since the Hollomon equation does not generally describe well the strain-strain curve of austenitic stainless steels, the Voce equation is commonly used instead of the Hollomon equation, which has mostly been used for the traditional low-carbon Al-killed steels. They seem to obey it fairly well, except at the early stages of straining close to the yield point Samuel (2006). Evaluation of the limit strains in FLD can be accomplished from Eq. (7) by using the Levy-Mises (or Prandtl-Reuss) equations, from which one obtains the values for the limit strains ε_1* and ε_2 *, when the principal stress ratio $\alpha = \sigma_2/\sigma_1$ varies, for example, from 0 to 1.

Some experimental results for steel AISI 304 together with calculated necking limits based on various uniaxial and biaxial stress-strain curves are shown in Fig. 5. The composition of the steel is given in Table 1 (AISI 304 A). In-plane stretching was accomplished by using a flat-nosed 100 mm diameter punch and two separate supporting Marciniak-type driver strips between the punch and the deforming sheet to ensure straining in the flat punch nose area. It is clearly evident from Fig. 5 that stress-strain data strongly affects the calculated limit strains. Since the work-hardening depends strongly on both strain rate and temperature, the scatter is high. However, the measured limit strains are rather close to the calculated ones. In fact, from low-speed uniaxial tests it is possible to obtain much higher limits than from actual forming tests.

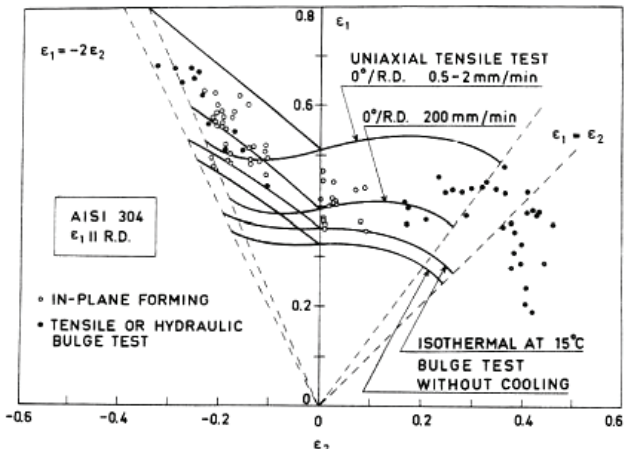

Table 1. Chemical composition of the steels (in mass %)

	AISI 304 A	AISI 304 B
C	0.06	0.038
Si	0.39	0.43
Mn	1.58	1.56
P	0.037	0.026
S	0.016	0.010
Cr	18.3	18.2
Ni	8.6	8.2
Mo	0.26	0.17
N_2	0.018	0.022

Figure 5. Comparison of calculated necking limits with the measured ones for steel 304 A (Korhonen, 1978b).

When the strain paths are not linear, the evaluation of the limit strains is still possible based on the

flow theory of plasticity (Korhonen, 1978a). The effective strain must be integrated along the path until the criterion given in Eq. (7) is met. Thus, the general necking criterion takes the form

$$\bar{\varepsilon} = \int d\bar{\varepsilon} \approx \sum \Delta\bar{\varepsilon} = \bar{\varepsilon}^{*}. \qquad (8)$$

Fig. 6 shows some experimental results with steel AISI 304 A on two simple strain paths consisting of just two parts. In this case the effective limit stain in equibiaxial tension was $\bar{\varepsilon}^{*} = 0.804$, while on the corresponding two-stage path shown in Fig. 6 a slightly larger value of $\bar{\varepsilon}^{*} = 0.939$ was obtained. The difference is hardly unexpected, taking into account the simplifying assumptions (Hill's yield criterion and isotropic work-hardening).

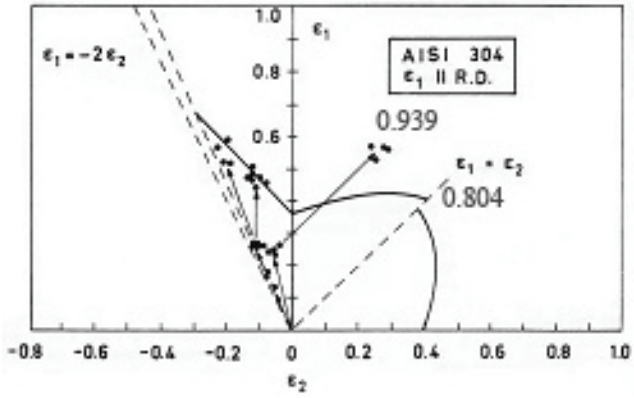

Figure 6. Experimentally measured limit strains for two strains paths consisting of two stages (Korhonen, 1978b).

2.2. Experimental observation of failed specimens

Two different commercially available austenitic stainless steels obtained from two different producers were used in the experiments. They are denoted by A and B and had thicknesses of 1 mm and 0.8 mm, respectively. Their chemical composition is given in Table 1.

The experiments were carried out using a hydraulic bulge device with various circular and elliptic apertures. The diameters of the circular aperture were 50 mm and 100 mm. Deep drawing experiments were carried out using a hydraulic double-action (3 MN / 2 MN) press.

Figs 7 and 8 show examples of failed steels A and B after bulge and deep drawing tests, respectively. It appears that the failure takes place by shearing at an angle inclined to the through thickness direction and that no localized necking or thinning is observed in either case. There appear to be two competing shear fracture directions both inclined about 45 degrees to the through thickness direction.

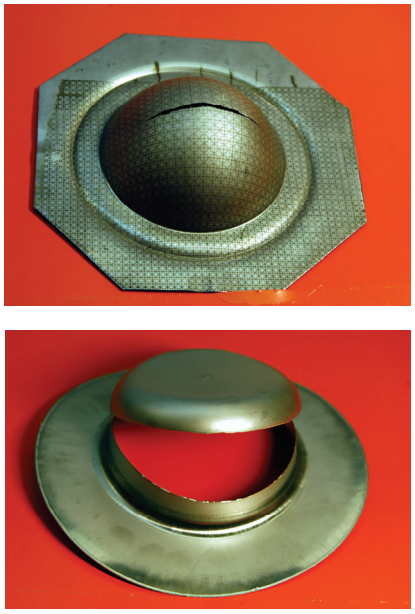

Figure 7. a) Failed steel 304 A after equibiaxial bulging above) and b) steel 304 B after deep drawing with cylindrical punch (below).

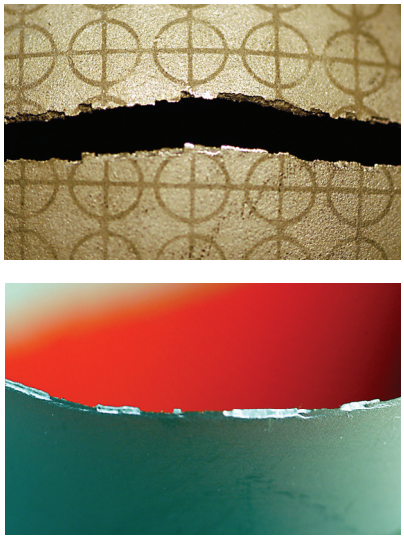

Figure 8. a) Detail of failed steel 304 A after equibiaxial bulging (above) and b) steel B after deep drawing with a cylindrical punch (below).

More details can be observed in SEM. Fig. 9 shows results for the deep drawn cup of steel B. The competing intersecting shear planes are clearly visible in Fig. 9 a), while a typical dimple pattern with some elongated ones as a result of shearing are seen in Fig. 9 b).

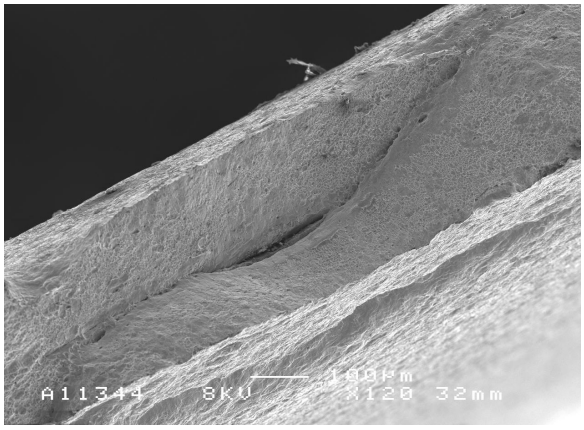

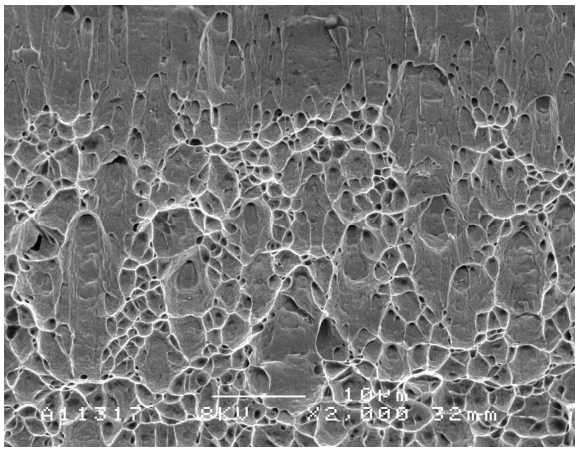

Figure 9. a) Failed steel 304 B after deep drawing with a cylindrical punch. Two intersecting shear planes (up) and b) a typical dimple pattern with some sheared and elongated ones (down).

3. FRACTURE OF TiN-COATED STAINLESS STEEL

Various coated stainless steels have been commercially available for many years. Physically vapor-deposited TiN and its variants TiAlN and TiAlCN were introduced by Nakamoto et al. (1993) to retain the original metallic finish but modify the color of the surface of stainless steel. According to their results, peeling of the TiN coating was not observed in deep drawing tests and the limiting drawing ratio of 2.2 was not affected by the thin hard coating.

Eriksson et al. (1992) and Pischow et al. (1994) carried out tests on formed 304 stainless steel parts, which were coated with TiN either before or after forming. A gold-colored TiN coating was deposited on austenitic stainless steel tensile test specimens and blanks, which were subsequently deformed by hydraulic bulging and by carrying out LDH tests. The TiN coatings were deposited by triode ion plating based on high-voltage electron beam evaporation of titanium into a nitrogen atmosphere. No peeling of the TiN was observed during forming. Hydraulically bulged TiN-coated stainless steel samples were tested for corrosion and even with the TiN-coated and subsequently formed samples their corrosion resistance remained good despite the small cracks visible on the surface.

Fig. 10 shows how the TiN coating on AISI 304 stainless steel behaves with increasing straining (Korhonen and Eriksson, 1994; Eriksson et al., 1992). With thicker coatings, brittle cracks perpendicular to the tensile axis appear first. After continued straining the hard coating tries to accommodate the gross plastic deformation by shearing cracks inclined to the tensile axes appear. These are approximately in the direction of zero direct strain, which for isotropic materials would be 54.7° away from the tensile axis.

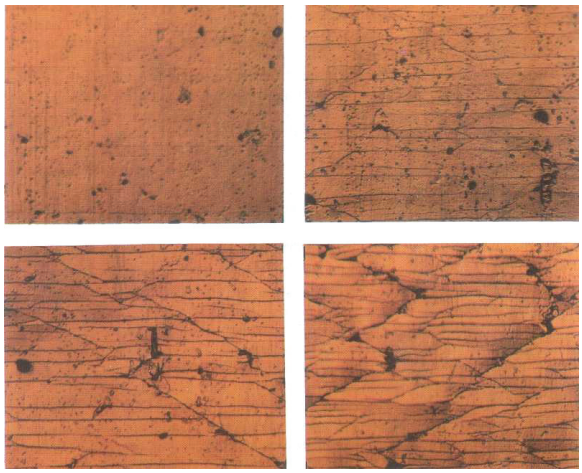

Figure 10. 4 μm thick TiN coatings on 304 steel after 2, 4, 10 and 20 % uniaxial tensile straining (Eriksson et al.,1992; Korhonen and Eriksson, 1994).

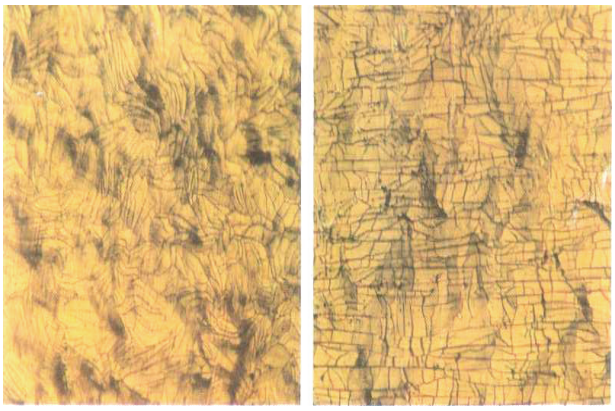

Figure 11. 1 μm thick TiN coatings on 304 stainless steel after a) hydraulic bulging and b) LDH test (Korhonen and Eriksson, 1994).

Fig. 11 shows an example of fracture patterns observed in TiN-coated stainless steel after hydraulic bulging and LDH testing, respectively. After equibiaxial bulging with no friction between the sheet and the hydraulic fluid there appears to be no

clear directionality in the crack pattern, while after punch stretching in the LDH test pronounced cracking perpendicular to the largest principal stress direction can be clearly seen.

4. DISCUSSION

The experimental results show that on the right-hand side of the FLD austenitic stainless steel tends to fail by shearing rather than local necking or thinning. The observed dimple pattern in the SEM micrographs is typical of ductile fracture. In tensile testing they were first observed by Rogers (1960), who suggested that they result from internal cracking starting from voids created on second phase particles.

The fact that there appears to be no local necks or thinning may be explained by the strong work hardening ability of the austenitic stainless steels. On the left-hand side of the FLD, however, both diffuse and local necking are observed, e.g. in tensile testing.

Depending on the strain path, the forming limits may either increase or decrease. Assuming that the effective limit strain is a function only of some material parameters and the final stress ratio of the strain path, this can be easily understood. In the case of Hollomon and Voce equations one obtains the results shown in Eqs. (6) and (7) for either diffuse or local necking limit strain. However, although $Z = Z(\alpha)$, where $\alpha = \sigma_2/\sigma_1$ for Hill's yield condition, this is not necessarily the case for all other possible hardening laws and yield functions f (see Eqs. (1) to (3)). The stress-based FLD was first proposed by Arrieux et al. (1982) and more recently supported by Stoughton (2002) with additional experimental evidence provided by Kuwabara (2005) and Yoshida et al. (2005).

There are many models for ductile fracture and new ones are being developed. Some of them have been recently reviewed and compared by Bao and Wierzbicki (2004). They state that despite the improvements introduced later by e.g. Tvergaard and Needleman and others, the well-known Gurson model still includes ten parameters which are difficult to calibrate. Other industrially difficult models include e.g. the damage mechanics based model of Kachanov and its thermodynamic potential based derivatives. Equally difficult, despite its popularity, seems to be the cohesive zone model introduced by Barenblatt and Hillerborg et al. Due to these difficulties Bao and Wierzbicki chose nine simple ductile fracture criteria for their experimental study. These were the criteria of effective strain, Cockroft-Latham-Oh, hydrostatic stress, Clift, Brozzo, Rice-Tracey high stress triaxiality approximation, General Rice-Tracey, LeRoy and McClintock.

The stress-based FLD or stress-space FLD (SSFLD) concept neglects the effect of hydrostatic stress to forming limits. Although this may be feasible, when isotropic hardening and necking is considered, it certainly is not when fracture determines the forming limit. For example, in the earlier cited experiments with extruded aluminum tubes (Kuwabara, 2005; Yoshida et al., 2005) no signs of necking are visible in fractured tubes. In fact, the shape of the SSFLD resembles a section of the Tresca yield condition in the first quadrant. Interestingly, Huber was already thinking about fracture when he published the criterion which later was conceived mathematically by von Mises and became known as the Huber – von Mises – Hencky yield condition (Engel, 1994). Recently, even a simple method for determining the SSFLD from a uniaxial tensile test has been proposed (Martin et al., 2006). However, it is well-known that the hydrostatic pressure affects fracture although yielding is often considered pressure independent. Thus, von Mises type of yield criteria have been commonly used, while for fracture Coulomb – Mohr type of criteria have been commonly used. For steels which undergo deformation-induced phase transformation during forming the assumption of hydrostatic pressure independent yielding and volume constancy may no longer be valid. However, due to the low carbon content of austenitic stainless steels the volume change associated with the martensitic phase transformation remains small.

Ritchie and Thompson (1985) presented a ductile fracture model based on the work of Rice and Tracey. Assuming the distance of void initiating defects to be twice their diameter, one obtains for the fracture strain

$$\bar{\varepsilon}_f = 2.48 \exp(-1.5\, \sigma_m / \bar{\sigma}), \qquad (9)$$

where σ_m is the hydrostatic stress. Fig. 12 shows some results. Based on the measurements made for steel AISI 304 A in Table 1 the coefficients of Voce's equation $\bar{\sigma} = B - (B - A) \exp(-n\bar{\varepsilon})$ were taken as A = 345 MPa, B = 1400 MPa and n = 1.85.

Although the fracture limit seems reasonably similar to the one already measured by several authors, it is still well above the limit strains reported in this work for the right-hand side of the FLD.

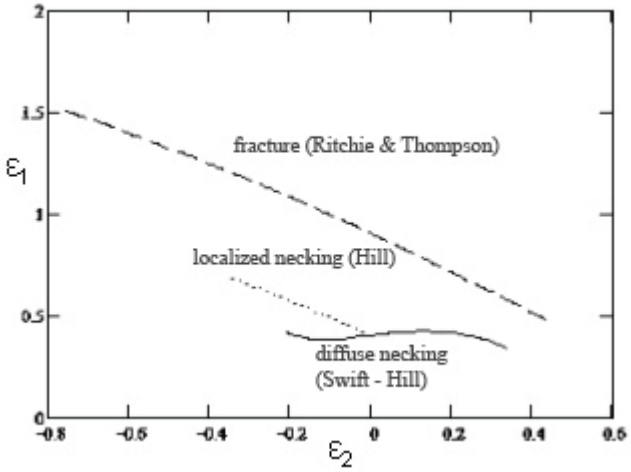

Figure 12. Comparison of calculated diffuse and local necking and fracture limits for steel 304 A

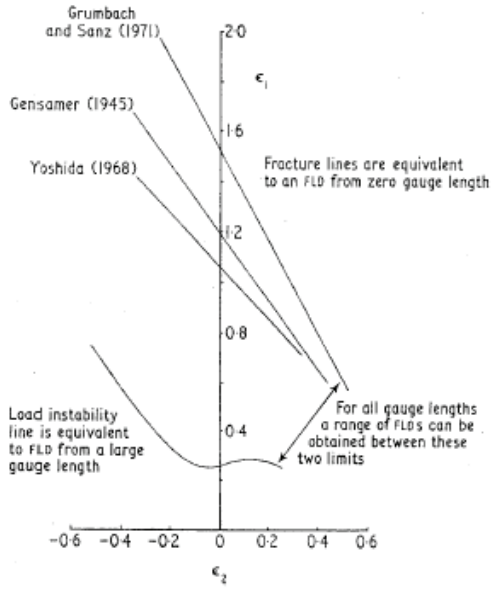

Figure 13. Comparison forming limits measured by various authors. (After Painter and Pearce, 1974).

Also the necking strains calculated for the given values of Voce's equation are high. The assumed distance of the void nucleation sites was probably too small as well, which makes the situation even worse. For some other softer metallic materials showing more pronounced localized necking the agreement may be better. Qualitatively the results seem to agree with the previous experimental observations, including the early work of Gensamer (1946). Fig. 13 shows a comparison of the forming limits measured by various authors according to Painter and Pearce (1974). It illustrates the fact that, depending on the amount of diffuse necking that precedes local necking or fracture, the grid size that is used for measuring the limit strains may lead to a great scatter in limit strain values. In this work it appeared that the limit strains for austenitic stainless steel on the right hand side of the FLD were determined by a shearing type of fracture inclined about 45° to the through thickness direction and not by localized necking, as is commonly observed e.g. for low carbon steels. The two mechanisms are illustrated schematically in Fig. 14. It is clear that the M-K type of analysis of failure and prediction of forming limits in stretch forming is not valid if the failure takes place by shearing rather than by necking. Recently, McGinty and McDowell (2004) have shown that by using a crystal plasticity based hardening law many different shapes of forming limit curves can be obtained. However, association of the M-K type necking criterion is not valid if the failure takes place by shearing instead of necking.

The formability of austenitic stainless steels seems to be generally very good. Even a hard ceramic coating such as TiN on top seems not to affect their formability greatly. Adhesion of the TiN coating produced by using modern physical vapor deposition techniques such as ion plating and sputtering seems to be very good. However, cracking seems to be unavoidable in severely formed parts and the observed crack patterns are affected by the stress state. K_I type of cracking perpendicular to the highest principal stress is commonly observed first, followed by inclined shearing to accommodate the continuing plastic straining. Although the corrosion resistance seems to remain good, cracking of the hard coating obviously limits the application of forming to TiN coated sheets.

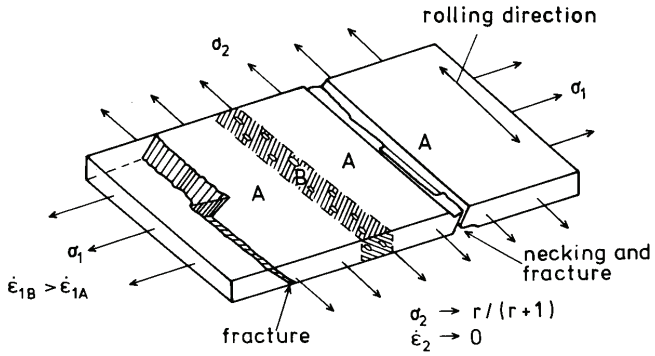

Figure 14. Schematic illustration of shearing and necking type fractures (Korhonen, 1978a).

It appears that on the right-hand side of the FLD the diffuse necking or load maximum instability criterion may be used to predict the limit strain. However, the results show great scatter, since work hardening of metastable austenitic stainless steels depends strongly both on strain rate and temperature. Better hardening models are needed to describe work hardening of austenitic stainless steels more

accurately and to develop good criteria to predict their forming limits.

5. SUMMARY AND CONCLUSIONS

The formability of austenitic stainless steels and various models for the prediction of their forming limits were reviewed. It appeared that the forming limits in stretch forming are not set by localized necking but rather by sudden shearing in a direction inclined to through thickness direction. The formation of voids was observed inside the shear bands. Due to the absence of visible necks on the right-hand side of the FLD, a Marciniak – Kuczynski type of analysis cannot be used to predict the limit strains. A diffuse necking or load maximum based instability criterion seemed to predict the limit strains on the right-hand side rather well. The problem, however, is that the work hardening depends strongly on both strain rate and temperature, and causes great scatter in the calculated limit strain values. The stress-based forming limit criteria seem to neglect the dependence of fracture of the hydrostatic pressure. The criterion presented by Ritchie and Thompson was used to calculate the limit strains and to predict the fracture limit. It appears the model overestimates the fracture limit considerably for austenitic stainless steels, but shows a correct trend observed in many earlier studies for other metals which exhibit necking behavior.

The formability of austenitic stainless steels appears to be good and even steels coated with a hard ceramic coating such as TiN may be successfully formed. However, cracking of such a hard coating may limit the application of forming of such coated steels. More information is needed on the work-hardening behavior of metastable austenitic stainless steels to develop better models to predict their behavior in forming and to estimate their forming limits more accurately.

REFERENCES

Andersson, R., Schedin, E., Magnusson, C., Ocklund, J., Persson, A., 2002, The Applicability of Stainless Steels for Crash Absorbing Components, SAE Technical Paper 2002 -01-2020, *Int. Body Engineering Conference & Exhibition and Automotive & Transportation Technology Congress*, Paris, Society of Automotive Engineers.

Arrieux, R., Bedrin, C., Boivin, M., 1982, Determination of an intrinsic forming limit stress diagram for isotropic metal sheets, *12th IDDRG Biennial Meeting*, S. Margherita Ligure, Working Group Meetings, WG I, 61-71.

Bao, Y., Wierzbicki, T., 2004, A Comparative Study on Various Ductile Crack Formation Criteria, *J. Eng. Mater. Techn*., 126, July, 314-324.

Chow, C. L., Jie, M., Wu, X., 2005, Localized Necking Criterion for Strain-Softening Materials, *J. Eng. Mater. Techn*., 127, 273-278.

Col, A., 2005, Forming limit curves: are we at the turn?, *Proc. 24th IDDRG Congress*, Besançon, Paper No. 18.

Engel, Z., 1994, Historical Aspects of Huber's Work, in *Huber's Yield Criterion in Plasticity*, eds, Pietrzyk, M., Kusiak, J., Sadok, L., Engel, Z., Akademia Górniczo-Hutnicza, Kraków, 1-7.

Eriksson, L., Harju, E., Korhonen, A. S., Pischow, K., 1992, Formability and corrosion resistance of TiN-coated stainless steel sheet, *Surface and Coatings Technology*, 53, 153-160.

Ferreira, P.J., Vander Sande, J.B., Amaral Fortes, M., Kyröläinen, A., 2004, Microstructure Development during High-Velocity Deformation, *Metall. Mater. Trans*. 35A, 3091 – 3101.

Gensamer, M., 1946, Strength and ductility, *Trans. Am. Soc. Metals*, 36, 30-60.

Habara, Y., 2004, Stainless Steel 200 Series: An Opportunity for Mn, in *International Manganese Institute Annual Conference*, Tokyo. http://www.manganese.org/2004AC_Presentations.php

Hill, R., 1952, On the discontinuous plastic states, with a special reference to localized necking in thin sheets, *J. Mech. Phys. Solids*, 1, 19-30.

Hill, R., 1957a, On the problem of uniqueness in the theory of rigid-plastic solid – III, *J. Mech. Phys. Solids*, 5, 153-161.

Hill, R., 1957b, Stability of rigid-plastic solid, *J. Mech. Phys. Solids*, 6, 1-8.

ISSF, 2005, "New 200-series" steels: An Opportunity or threat to the image of stainless steel?, *International Stainless Steel Forum (ISSF)*, 14. http://www.worldstainless.org/articles/200series.pdf

Jeswiet, J., Micari, F., Hirt, G., Bramley, A., Duflou, J., Allwood, J., 2005, Asymmetric Single Point Incremental Forming of Sheet Metal, *Annals of the CIRP*, 54, 2, 623-649.

Kemppainen, J., 2000, Stainless Steel – A New "Light Metal" for the Automotive Industry, Stainless Steel in Structural Automotive Applications – Properties and Case Studies, *Paris Motor Show Mondial de l'Automobile, Euro Inox*, The European Stainless Steel Development Association, 3. http://www.euro-inox.org/

Kemppainen, J., Schedin, E., Sörqvist, E., 2002, HyTens Creates New Opportunities for High Strength Stainless Steel Applications, *Acom,* 3/4, 2–6.

Kleemola, H. J., Pelkkikangas, M., 1977, Effect of predeformation and strain path on the forming limits of steel, copper and brass, *Sheet Metal Industries*, 54, 591-599.

Korhonen, A. S., 1978a, On the Theories of Sheet Metal Necking and Forming Limits, *J. Eng. Mater. Techn*., 100, 303-309.

Korhonen, A.S., 1978b, On the Work-hardening and Formability of Austenitic StainlessSteels, *Sheet Metal Industries*, 55, 5, 598-606.

Korhonen, A. S., 1980, Localization of plastic flow and ductile fracture in metals, Acta Polytechnica Scandinavica Ch 144, 33 p.

Korhonen, A. S., Eriksson, L., 1994, On the plastic flow and fracture of metals and hard coatings, in *Huber's Yield Criterion in Plasticity*, eds, Pietrzyk, M., Kusiak, J., Sa-

dok, L., Engel, Z., Akademia Górniczo-Hutnicza, Kraków, 293-303.
Kuwabara, T., 2005, Advances of Plasticity Experiments on Metal Sheets and Tubes and their Applications to Constitutive Modeling, *Proc. Numisheet 2005, AIP Conf. Proc*., Vol. 778, 20-39.
Lademo, O.-G., Pedersen, K. O., Berstad, T., Hopperstad, S., 2004, A numerical tool for formability analysis of aluminium alloys. Part II: Experimental validation, *Steel Grips 2, Suppl. Metal Forming 2004*, 433-437.
Lankford, W. T., Low, J. R., Gensamer, M., 1947, The Plastic Flow of Aluminum Sheet Under Combined Loads, *Trans. AIME*, 171, 574-604.
Makinouchi, A., Teodosiu, C., Nakagawa, T., 1998, Advance in FEM Simulation and its Related Technologies in Sheet Metal Forming, *Annals of the CIRP,* 47, 2, 641- 649.
Manninen, T., Larkiola, J., Korhonen, A. S., 2002, Modeling of deep drawing of stainless steel, in *Information Technology, Global Environment and Sheet Metal Forming, Proc. of the 22nd IDDRG Biennial Congress*, Nagoya, 43-49.
Martin, P. H., Smith, L. M., Petrusevski. S., 2006, A method for stress space forming limit diagram construction for aluminum alloys, *J. Mat. Proc. Techn*., 174, 258-265.
McGinty, R. D., McDowell, D. L., 2004, Application of Multiscale Crystal Plasticity Models to Forming Limit Diagrams, *J. Eng. Mater. Techn*,126, 285-291.
Müschenborn, W., Sonne, H.-M., 1975, Influence of the strain path on the forming limits of sheet metal, *Archiv für das Eisenhüttenwesen*, 46, 598-602.
Nakamoto, K., Shiotani, K., Makimoto, M., Saito, M., 1993, Development of Colored Stainless Steel Sheets by Ceramics Coating, *ISIJ Int*., 33, 968-975.
Painter, M. J., Pearce, R., 1974, Instability and fracture in sheet metal, *J. Phys. D: Appl. Phys*. 7, 992-1002.
Pischow, K. A., Eriksson, L., Korhonen, A. S., Forsén, O., Turkia, M., Ristolainen, E. O., 1994, Corrosion behavior of decorative car parts and outdoor lighting fixtures fabricated from TiN-coated stainless steel, *Surf. Coat. Techn*., 67, 85-93.
Ritchie, R. O., Thompson, A. W., 1985, On Macroscopic and Microscopic Analyses for Crack Initiation and Crack Growth Toughness in Ductile Alloys, Metall. Trans., 16A, 233-247.
Rogers, H. C., 1960, The tensile fracture of ductile metals, *Trans. Met. Soc. AIME*, 218, 491-506.
Samuel, K. G., 2006, Limitations of Hollomon and Ludwigson stress-strain relations in assessing the strain hardening parameters, *J. Phys. D: Applied Physics*, 39, 203-212.
Seth, M., Vohnout, V. J., Daehn, G. S., 2005, Formability of steel sheet in high velocity impact, *J. Mat. Proc. Techn*., 168, 390-400.
Stoughton, T. B., 2002, The Influence of the Material Model on the Stress-Based Forming Limit Criterion, *SAE 2002 World Congress & Exhibition*, Detroit, SAE Technical Paper No. 2002-01-157, 10.
Talonen, J., Nenonen, P., Hänninen, H., 2004, Static strain ageing of cold-worked austenitic stainless steel, *Proc. of the 7th Int. Conf. on High Nitrogen Steels, Steel Grips 2 (2004) Suppl. High Nitrogen Steels*, 113–122.
Talyan, V., Wagoner, R. H., Lee, J. K., 1998, Formability of Stainless Steel, *Metall. Mater. Trans*., 29A, 2161–2172.
Yagodzinskyy, Y., Pimenoff, J., Tarasenko, T., Romu, J., Nenonen, P., Hänninen, H., 2004, Grain Refinement Process for Superplastic Forming of AISI 301 and 304L Austenitic Stainless Steels, *Mat. Sci. Techn*., 20, 925–929.
Yoshida, K., Kuwabara, T., Narihara, K., Takahashi, S., 2005, Experimental Verification of the Path-Independence of Forming Limit Stresses, *Int J. Forming Proc., Special Issue 2005*, eds, Habraken, A.-M., Stören, S., 283-298.

ODKSZTAŁCALNOŚĆ BLACH ZE STALI AUSTENITYCZNEJ ODPORNEJ NA KOROZJĘ

Streszczenie

Przedmiotem pracy jest odkształcalność graniczna stali austenitycznych. Zaobserwowano, że odkształcalność prze dwuosiowym rozciąganiu, gdy dwa naprężenia główne są dodatnie, nie jest wyznaczana przez lokalne tworzenie się szyjki, ale przez pękanie wywołane przez ścinanie w kierunku grubości blachy. Dlatego metoda Marciniaka-Kuczynskiego, która jest z powodzeniem stosowana do stali nisko-węglowych i aluminium, może nie stosować się do stali austenitycznych. Okazuje się, że odkształcenia graniczne stali austenitycznych mogą być poprawnie przewidywane przez zastosowanie opracowanego przez Hilla klasycznego kryterium lokalizacji i rozprzestrzeniania się szyjki. Kryterium pękania Ritchie-Thompsona wydaje się przeszacowywać granicę pękania. Ponieważ umocnienie zależy mocno od prędkości odkształcenia i temperatury, lepsze modele są potrzebne do opisu umocnienia i opracowania poprawnego kryterium granicznych odkształceń. Odkształcalność graniczna stali austenitycznej utrzymuje się na dobrym poziomie nawet wtedy, gdy stal jest pokryta TiN, chociaż nieuniknione pęknięcia pojawią się w czasie odkształcenia.

Submitted: October 3, 2006
Submitted in a revised form: December 19, 2006
Accepted: December 19, 2006